Instrument: **SP1 Cooperation**

Thematic Priority: **Priority Area 1.1.6.3 "Global Change and Ecosystems"**

FP7 Collaborative Project – Grant Agreement 212492

CLARIS LPB
A Europe-South America Network for Climate Change Assessment and Impact Studies in La Plata Basin

DELIVERABLES

D9.13: Model of the geomorphology and sediments in the Lower Paranà River

Due date of deliverable: Month 30

Start date of project: **01/10/2008** Duration: 4 **years**

Organisation name of lead contractor for this deliverable: University of Bologna

Deliverable No	Deliverable title	WP	Lead beneficiary	Estimated indicative person-months (permanent staff)	Nature	Dissemination level	Delivery date
D9.13	Model of the geomorphology and sediments in the Lower Paranà River	9	P6-UNIBO	2,00	O	CO	30

Massimo Guerrero[(1)]
Maria Gabriella Gaeta[(1)]
Ricardo Szupiany[(2)]

[(1)]*Hydraulic Laboratory, University of Bologna, Bologna, Italy*
[(2)]*Cenro de Estudio de Grande Rios, Facultad de Ciencias Hídricas, Universidad National del Litoral, Santa Fe, Argentina*

Abstract

Concerning the climate of La Plata Basin the XX century can be subdivided in three period as reported by Garcia and Vargas, 1998, and Garcia et al. 2002 with a dry period of 40 years in the middle and wet periods at starting and closure of the century. In particular the precipitations had the same behaviour in the upper and lower basin therefore giving rise to the same streamflow tendency changes within the century. A near 30 year long period can be argued in the stream flow variability (i.e. interdecadal variability) that can be correlated to some climate indices (Maciel, Diaz and Terra, 2010). Furthermore some evidences exist that a certain increment of discharge starting from 1970-1971 was due to land use change on the Brazilian area of the basin, began in 1968 (Garcia et al. 2002). That increment differently summed with increased rainfall increment depending on La Plata Basin areas. In particular Doyle & Barros (2010) show as the run off increasing was caused by land use change in the north, by climate variability in the south and by both in the middle part of the basin. The same authors show as extreme events recurrence is not strongly correlated with interdecadal variability at Corrientes (northern par of Paranà River) meanwhile it appeared better correlated to hydrology-climate variability for the Uruguay River at Paso de los Libres. This occurrences bear out the evidence that streamflow increasing at Lower Paranà was mainly related to climate variability.

Amsler et al. (2005) quantitatively analyzed as the streamflow interdecadal variability affected the channel morphology of Paranà River in its middle reach during XX century, meanwhile Castro et al. (2007), carried out a similar study for a 50 km long reach at very beginning of lower Paranà between

Puerto San Martin and Alver (nearby Rosario City). The former study clearly correlate climate interdecadal variability to effective discharge (i.e. the discharge value most effective modifying the morphology) variability and as a consequence to river morphology changes. In particular the dry midst of the century (1930-1970) was characterized by low effective discharge that promoted a decrease in width , braided index, thalweg sinuosity, width to depth ratio and channel volume, vice versa for the century began and end. In other words, for middle Paranà, the dry period accomplished to reduce sediment transport and river channel planimetric dimensions while wet periods, on the contrary, increased sediment transport and enlarged river channel giving rise to islands formation within it. The lower Paranà morphodynamics is not straightforward correlated to hydrology variability as much as the middle Paranà. In particular historical cartography of the reach between San Martin and Rosario bears out a continuously and progressive oversimplification of river channel planimetric morphology toward a lower width to depth ratio, the last part of the century, since 1970, not recovering the extremely braided morphology that characterized the century begin, on the contrary exacerbating the midst century morphodynamics processes. This occurrence is not easy justified by hydrology interdecadal variability therefore the authors found additional reasons in the alluvial plane morphology that starting from San Martin up to the la Plata River strongly enlarge and decrease in slope. This morphology constrains together with increased effective discharge, during the last part of the century, would has produced sediment deposition at secondary reaches and therefore the streamflow gathering in a single straight and deep reach. As a matter of fact the authors report evidences on decreased water slope at effective discharge that is correlated to sediment deposition increasing.

Our contribute is aimed to clarify the lower Paranà morphodynamics during XX century in the light of mentioned interdecadal variability, morphology constrains and land use change. In particular we applied two wide accepted numerical models in the river engineers community. The HEC-RAS by US Army simulates river hydro-morphodynamics in one dimensional, 1D model (U.S. Army Corps of Engineers, 2008), therefore reproducing effective discharge, water surface and bed slopes changes in the whole

Paranà river from Corrientes to Villa Costitution (865 km). The MIKE 21C by Danish Hydraulic Institute is a two dimensional, 2D, model (DHI Water and Environment, 2002) that was applied to the more upstream part, 24 km long, of the lower Paranà reach that was studied by Castro et al. 2007 (i.e. from San Martin to Rosario bridge). This model is able to simulate local deposition and therefore river channel tendency towards braided or meandering single channel configuration.

The river cross-sections for 1D model comes from 70's topographic survey by INA, we calibrated the model by comparing water level at 18 stage measurement in the period 1994-1999 and adjusting bed roughness and floodplain width, herein simulated as part of cross-section with reduced velocity. The calibration of sediment transport formula for bed sand was carried out by means of 1D model considering the documented bed slope change and the other available historical data and the filed campaign that we carried out at San Martin-Rosario reach in 2009 and 2010.

The 1D model was useful to simulate the whole XX century hydraulics and therefore reproduce the related effective discharge variability both at middle and lower Paranà. Furthermore we verified the water and related bed slope changes during the last part of the century (1970-2010) by mean of a morphodynamic simulation. The 1D model results also supplies boundary conditions for 2D model morphodynamic simulations of the period 1954-1976. A separate analysis was carried out by means of 1D model on wash load advection-dispersion process that takes place from Bermejo sub-basin to Paranà delta incoming, aiming to quantify delta front future advancement.

We surveyed the channel bathymetry for 2D model in 2009 together with suspended sediment transport and velocity field using acoustic Doppler current profilers (ADCP) and single beam echosounder. The hydraulic calibration of the 2D model was carried out on 2009 survey steady conditions, therefore adjusting bed roughness as calibration parameter. The 2009 bathymetry was then modified in agreement with midst century channel margins and Castro et al. 2007 morphology analysis concerning river channel volume, depth and width. Therefore, applying the morphodynamic module of MIK21C, we carried out a sensitivity analysis on sediment transport lateral deviation with the aim to reproduce the channel morphology changes that were observed in the first part of the second half of the century (i.e., 1954-1976). This analysis bear out the river mechanisms that were fostered by climate and land use changes by means of changed regime of effective discharge.

Introduction

The Lower Paranà morphodynamics is not straightforward correlated to hydrology variability. According to Garcia & Vargas (1998) and Garcia et al (2002) streamflow and precipitations have the same tendency variations during the XX century, in particular a dry period of nearly 40 years was observed in the basin in the midst of the century.

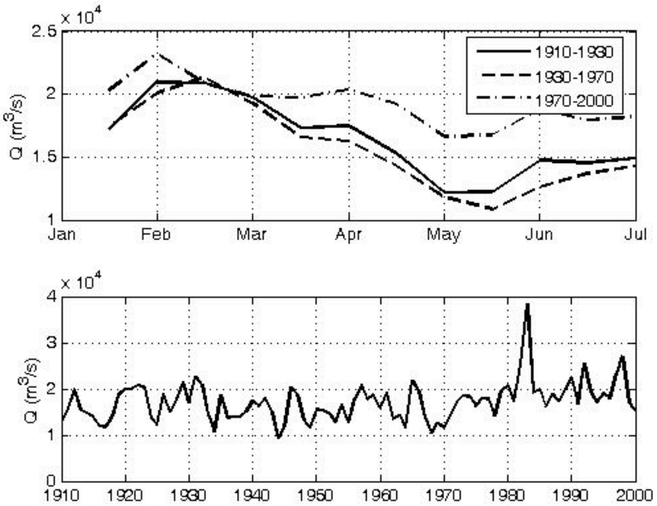

Figure 1 Monthly average for 3 decades and yearly discharges at Corrientes for the XX century.

Notwithstanding the hydrology change and land use change beginning around 1970 that consistently increased the Lower Paranà streamflow, historical cartography of the reach between San Martin and Rosario, reported in Figure 2, bears out a continuously and progressive oversimplification of river channel planimetric morphology toward a lower width to depth ratio, the last part of the century, since 1970, not recovering the extremely braided morphology that characterized the century begin corresponding to humid period, on the contrary exacerbating the morphodynamics processes occurring in the midst of the century (i.e., dry period).

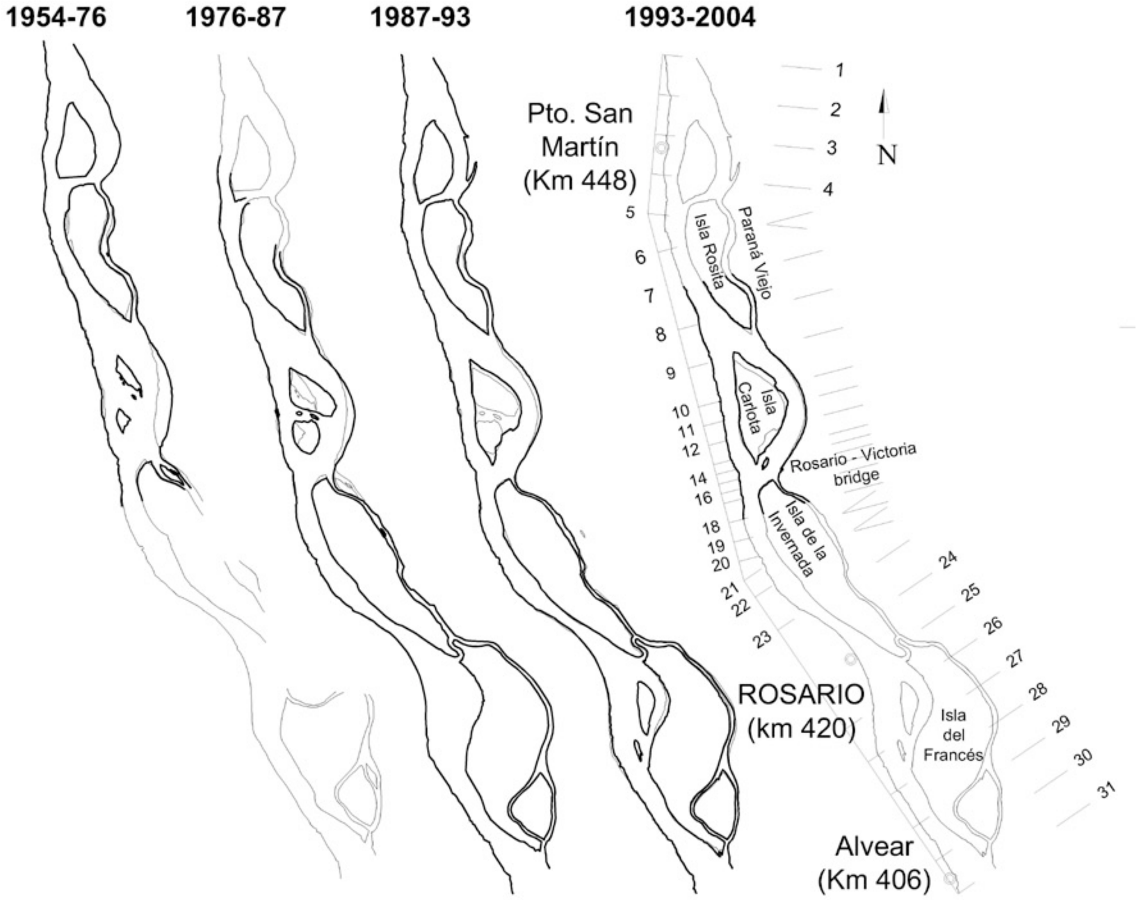

Figure 2 Margin comparisons at Lower Paranà reach in the XX century.

The Lower Paranà reach between Rosario and San Martin is also a strategic area for inner navigation because of the ports that are located along the river right bank where oceanic boats finally stop their upstream sailing along the Paranà-Paraguay water way (Figure 3).

Figure 3 Paranà-Paraguay water way.

These features drive our attention on the morphology singularities of the areas as the bifurcations and junction that are recognized as key features for river channel morphology development.

Therefore we carried out a detailed study of the fluvial processes observed in the upstream 24 km of the Lower Paranà reach in Figure 2, including the Carlota island within river cross-sections 9-14, with the final aim to validate the horizontal two dimensional (2D) numerical model, MIKE21C, by Danish Hydraulic Institute, 2002, then to be applied for the prediction of future morphology scenarios. MIKE21C is able to simulate long terms changes of river channel morphology also related to hydrology-climate change and affecting the thalweg displacement and navigation way maintenance. In particular we preliminary carried out the validation of the US Army, 2008, one dimensional (1D) numerical model, HEC-RAS, that was applied to the Paranà-Paraguay rivers system with the following aims: 1) to calibrate river bed sediment transport formulas at basin scale for river bed slope change prediction, 2) to supply MIKE21C with boundary conditions in terms of effective discharge, 3) to propagate wash load from Bermejo Basin to delta incoming for delta growth prediction.

Survey activities were carried out at the 24 km long reach case study. In particular we completed three field campaigns, June-July 2009, August 2009 and November 2010, using a single beam ecosounder, three Acoustic Current Doppler Profiler (ADCP), a water-suspended sediment sampler; all the instruments were real-time referenced with a RTK-GPS. The campaigns accomplished the following objectives: 1) to survey the current bathymetry for 2D model implementation; 2) to survey velocity field and sediment transport for the calibrations of 2D model.

Finally, the calibration of 2D numerical model include 1) the hydrodynamic and sediment transport calibrations on the whole 24 km long reach, within river cross-sections 1-14, Figure 2, using the 2009 observed morphology, velocity and suspended sediment features and the corresponding hydrology conditions, 2) the morphodynamic calibration on the 11 km long sub-reach, within river cross-sections 7-

14, Figure 2, aiming to reproduce the Carlota island formation processes occurred in the period 1954-1976.

Paranà river model

Aim of the 1D simulations is to validate a methodology to assess the impact of solid and liquid discharge regime change on river bed slope. In particular, hydraulic simulations of the Paranà basin in unsteady condition are carried out for the period 1970-2000, accomplishing the model calibration in terms of bed roughness and floodplain width. The validated model is then used as the base for the following morphological study, among two past periods characterized by opposite hydraulic behaviors, aiming to calibrate the sediment transport equation and to provide boundary conditions for the 2D model.

The model

HEC-RAS 4.0 by U.S. Army Corps of Engineers is one of the most widespread numerical models used to compute water-surface profiles and energy grade lines in one dimension (1D). It contains four river analysis components: steady-state and unsteady flow computation modules, sediment transport modelling in quasi-unsteady flow state and water quality analysis.

Fundamental hydraulics solved in the model is the continuity equation and energy equation by De-Saint Venant, solved using an implicit finite difference scheme:

$$\begin{aligned} &\frac{\partial A}{\partial t}+\frac{\partial Q}{\partial x}-q=0 \\ &\frac{\partial Q}{\partial t}+\frac{\partial (Q^2/A)}{\partial x}+gA\left(\frac{\partial h}{\partial x}+S_e+S_f\right)+\hat{Q}=0 \end{aligned} \qquad [1]$$

Energy losses are evaluated by friction S_f and contraction/ expansion S_e.

In the computations the model allows to include effects on the flow of various and common engineering obstructions, i.e. bridges, culverts, spillways and to model in unsteady state conditions storage areas and their hydraulic connections.

The updated version of the model has been implemented with the sediment transport module. Bed and suspended sediment transport are both reproduced in the model under quasi-steady flow regime, approximating a continuous hydrograph with a series of discrete steady flow profiles.

The sediment transport capacity is computed for each grain size class constituting the bed material and for each computed control volume: the transport potential is computed with one of the commonly used transport equations, available in the model.

For this study, the Engelund-Hansen formula (1967) is chosen in the numerical model, giving the total bed transport rate, as:

$$g_s = 0.05 \cdot \gamma_w \cdot s \cdot V^2 \cdot \sqrt{\frac{d_f}{g \cdot (s-1)}} \cdot \left[\frac{\tau_\circ}{(\gamma_w \cdot s - \gamma_w) \cdot d_f}\right]^{\frac{3}{2}} \cdot B \qquad [2]$$

while, the evaluation of the fall velocity is performed using the van Rjin, 1984, expression.

The calculation simulates long-term trends of scour and deposition in stream channel.

The 1D model reproduces an almost 10'000 km^2 wide area of interest, including Paranà and Paraguay rivers (Figure 4).

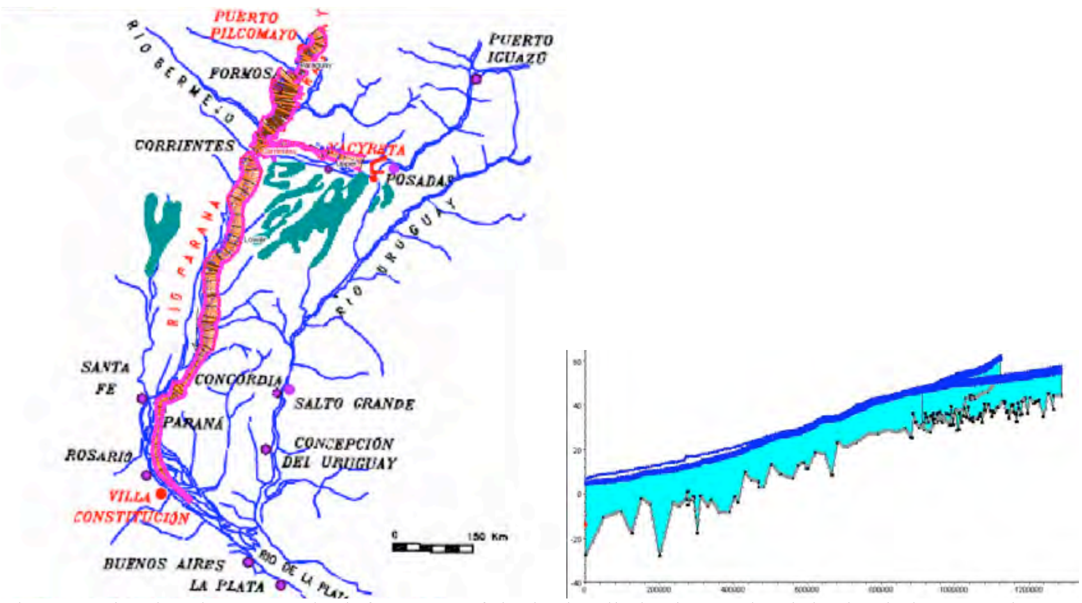

Figure 4 Simulated area: on the left, a map of the hydraulic basin, on the right the thalweg section as in the model.

In particular, Paraguay river is studied from Asuncion to Corrientes for a 375 km long reach, while Paranà river is studied for the 215 km long reach from Ituzaingò to Corrientes (i.e., Upper Paranà), where the two rivers merge, and for the 865 km long reach from Corrientes to Villa Constituciòn (i.e., Middle and Lower Paranà).

The hydraulic simulation

The analyzed period goes from 01.08.94 to 13.01.99 (233 weeks). The sections included in the numerical model are available thanks to previous studies and surveys performed by the Instituto Nacional de Agua (INA). In particular:

- the bathymetries in 76 cross sections along the reaches, derived from surveys carried out in 70's;

- the boundary conditions, the stage hydrographs at Villa Constitution and at Asuncion and the rating curve at Ituzaingò;

- the stage hydrographs, measured in 18 stations (Table 1): 2 for Paraguay and Upper Paranà and 14 for Middle-Lower Paranà. These measurements are used to calibrate and validate the numerical model.

Table 1 River cross-sections list where are stage hydrographs are available within the period 1994-1999.

#	Reach	Station	Prog Dist [km]
1	Paraguay	Formosa	169
2	Paraguay	Bermejo	311
1	U. Paranà	Ita Ibaté	74
2	U. Paranà	Itatí	175
1	Paranà	Corrientes	246
2	Paranà	Empedrado	315
3	Paranà	Bella Vista	397
4	Paranà	Goya	482
5	Paranà	Reconquista	506
6	Paranà	Esquina	601
7	Paranà	La Paz	697
8	Paranà	Hernandarias	765
9	Paranà	Santa Fe	858.5
10	Paranà	Paraná	859
11	Paranà	Diamante	919
12	Paranà	San Lorenzo	1003
13	Paranà	Rosario	1033
14	Paranà	Villa Constitución	1083

The model is firstly implemented including as numerical domain the 76 sections of the interested area. Because of model stability requirements, the simulations are performed on a domain containing equally distant (4.0 km) and interpolated sections and setting a constant calculation time step equal to 1 hour. Bed roughness for the river channel and floodplain and the width of floodplain, not accurately represented in the model because of their 2D features, are evaluated as calibration parameters and adjusted in order to achieve a good agreement with measured levels.

The final numerical results of the 1D simulation are here presented only for three sections of interest at Middle-Lower Paranà: respectively, Rosario (downstream), Santa Fe (intermediate) and Corrientes (upstream).

Figure 5 shows the numerical domain for 1D Hec-Ras model and the cross sections of interest.

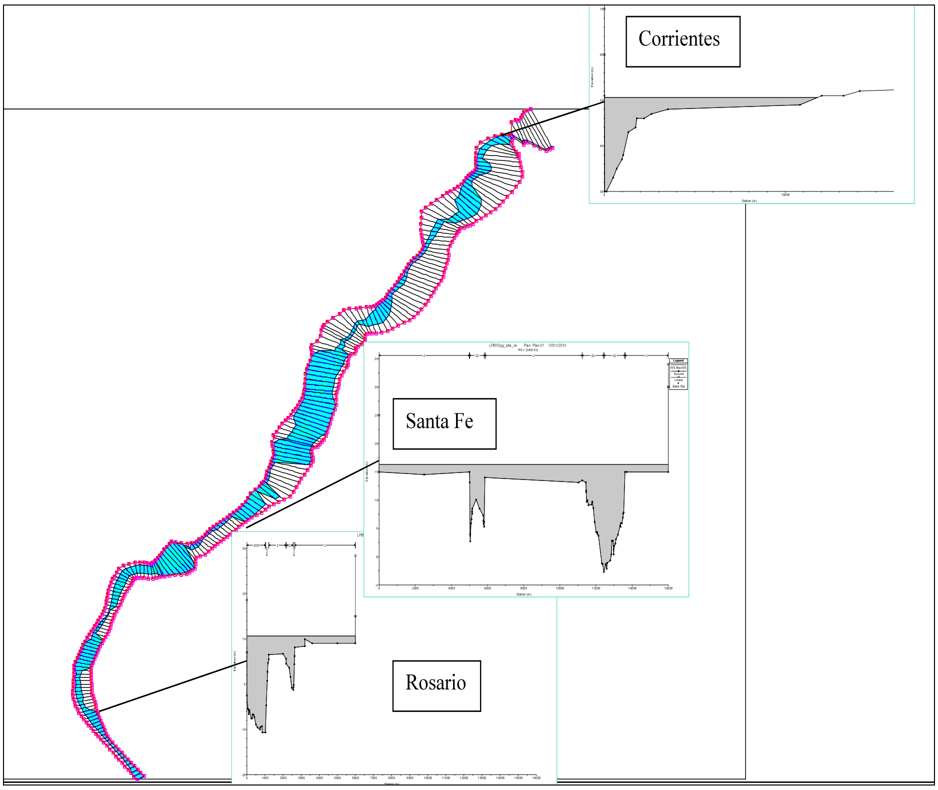

Figure 5 The computed Paranà river and the three studied sections at Corrientes, Santa Fe and Rosario.

The model requires upstream and downstream boundaries conditions: stage hydrographs were implemented both for the upstream condition at Paraguay river and at model downstream end in Villa Constituciòn (Lower Paranà), meanwhile the rating scale is used as upstream condition at Upper Paranà.

The section at Corrientes is common to all the 3 reaches, therefore it is defined in the model as a junction inner condition.

The initial conditions are derived performing a steady state flow analysis for the same geometric configuration.

The period between 01.08.94 and 31.07.95 is taken as calibration period, while the following period to 13.01.99 is used as validation.

The resulting distribution of calibrated river channel roughness is reported in Figure 6 as Manning coefficient *n* (top for Paraguay, middle for Upper Paranà, and bottom for Middle-Lower Paranà). Totally, the values are between 0.015 and 0.035 s/m$^{1/3}$.

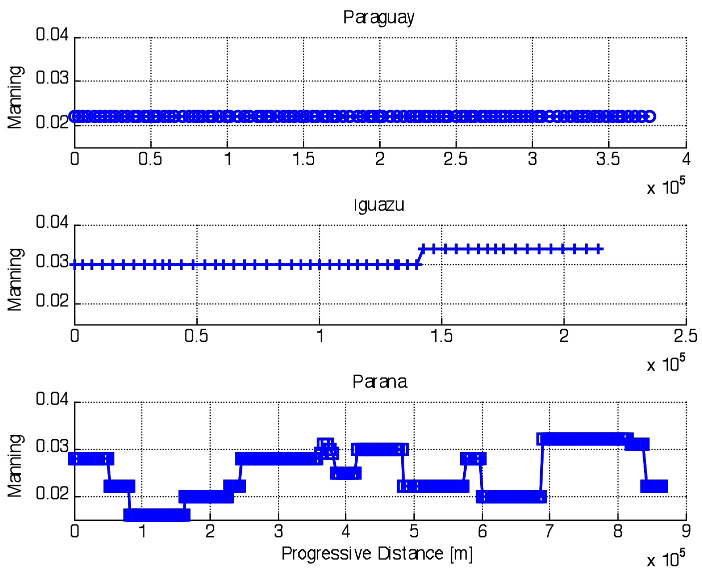

Figure 6 Distribution along simulated reaches of the Manning coefficient for river channel roughness.

Once the model is calibrated, the whole period 01.08.94 to 13.01.99 is simulated and the numerical results in terms of hydrographs are compared with the correspondent measurements at the 18 stations presented in Table 1. The comparisons achieve a very good agreement (Figure 7) in the three reaches. Some discrepancies arise during floods in sections where the floodplain configuration has two dimensions affecting the river hydrodynamics.

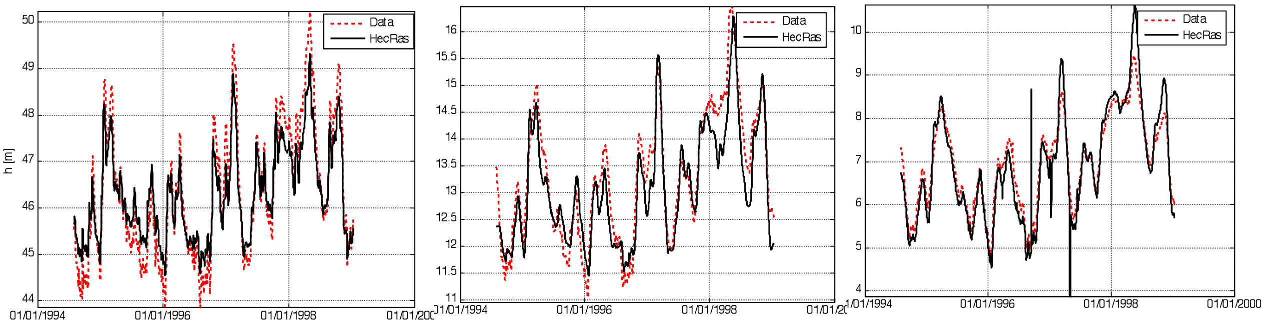

Figure 7 Comparison of water elevation hydrograph for Corrientes, Santa Fe and Rosario (from left to right); measured values are red dotted lines, and 1D model results are black solid lines.

The model validation is also performed by means of discharge value analysis.

At Corrientes, the rating curve is mathematically defined as follows from a study carried out by EVARSA S.A. based on a 15 year long period of data:

$$Q(y) = 0.44 \cdot (y + 12036)^{3.82} \qquad y \leq 22m$$
$$Q(y) = 567.22y^2 + 348.86y + 5393.5 \qquad y > 22m \qquad [3]$$

where y (m) is the stage level. The discharge values corresponding to simulated water levels by means of the Equation 3 are strongly correlated to 1D model values of discharge, correlation coefficient equal to 0.996, as is also evident in Figure 8.

Also the mean water slope results in reasonably values: around 2 cm/km for Paraguay river and Lower Paranà, and near to 4 cm/km for Upper-Medium Paranà.

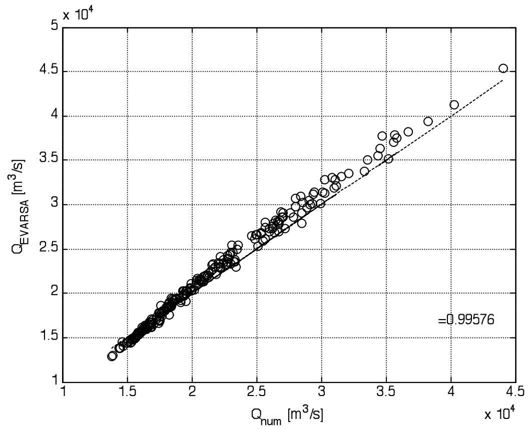

Figure 8 Comparison at Corrientes between the discharges calculated using Eq. [3] by EVARSA and the computed discharge from Hec-Ras model.

Using the validated model, we analyzed the river hydrodynamics during the simulated period. The following figures show the rating curve characterizing the three already mentioned cross-sections:

Corrientes, Santa Fe and Rosario. The computed data, re-sampled with a time step equal to 1 week, are here reported with the plus symbol, while the fitting curve is shown in the graphs as red solid line.

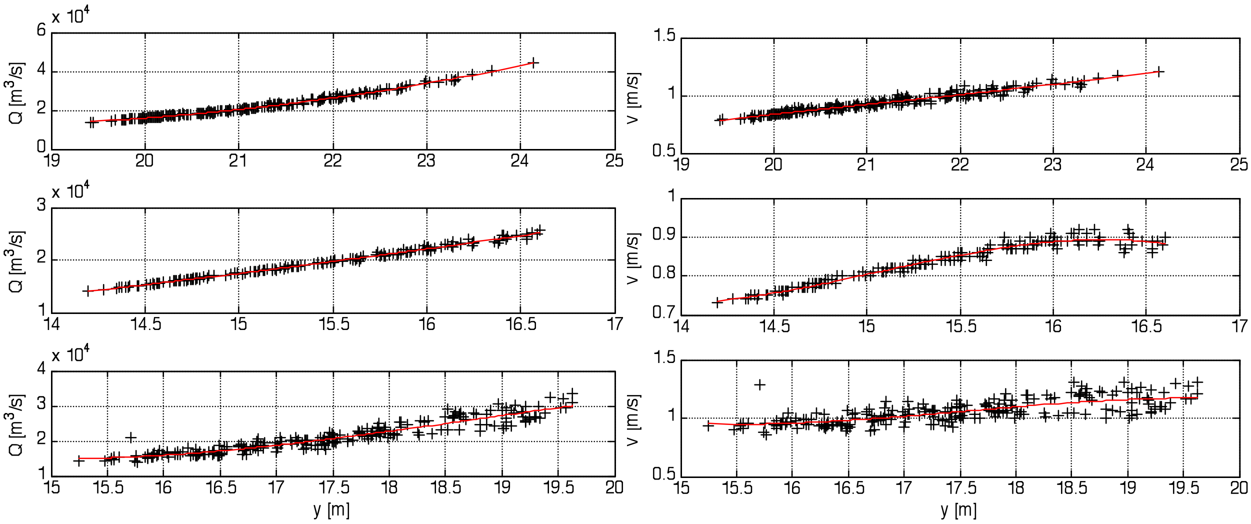

Figure 9 On the left, discharge versus stage; on the right, average velocity versus stage (points for computations and solid line for fitting) for Corrientes, Santa Fe and Rosario cross-sections (from above to below).

In Figure 9, the rating curves (left) follow a monotonic cubic law, as well as for the laws between the mean velocity-stage relations. One exception is represented by the Santa Fe cross-section where a maximal velocity remains constant for level higher than 16 m, probably due to its composite geometry (see Figure 5).

Wash load transport

Rio de la Plata is a very large estuarine system receiving waters of La Plata Basin. Its main tributary is the Paranà river that discharges through a broad delta, formed by deposition of upper basin sediments.

Paranà Delta is characterized by a continuous advancement process, with feed rates of several tens of meters per year and is protruding into the coast of Buenos Aires Province. The Delta dynamics implications on urban environment could be considerable, inducing conflicts between the nowadays uses at Rio de la Plata, i.e. final disposal of waste-waters, provision of drinking waters, navigation and recreation activities, etc.

The on-going climate changes will drive a different hydrological regime over Paranà basin, giving arise to sediment feeding modifications at the Delta and the consequent morphology adaptations affecting the mentioned human uses.

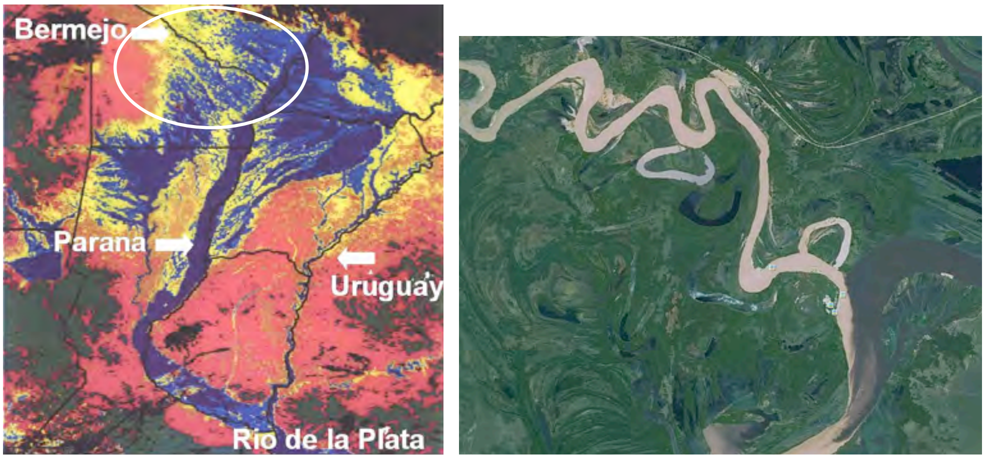

Figure 10 Satellite picture of LPB during 1998 flood and aerial picture of Bermejo junction. Note the different colour of Bermejo due to high suspended sediment load and its transport in Paranà reach.

Table 2 Annual suspended loads characterizing Paranà in the period 1995-2005 (Amsler et al., 2005).

Total suspended load for Paranà 150 mil ton/y		
Wash load (<50 µm) 135 mil ton/y		Bed/bank erosion 15 mil ton/y
from Bermejo 100 mil ton/y	rest of the basin 35 mil ton/y	

In order to predict this morphodynamics, fine sediment transport processes need to be investigated, since silts and clays partially settle during flood periods at the Delta islands. The sediment layer deposition and consolidation produce in time aggradation of the area.

After the validation of a tool for the prediction of sediment feeding at Paranà Delta in terms of concentration time series, the most probable future scenarios can be reproduce to predict future morphological changes.

In order to achieve the results, the 1D numerical model, previous calibrated in terms of hydrodynamics, is implemented to simulate the wash load transport at Paranà. In particular the proposed method propagates up to Rio de la Plata the sediment yield of Bermejo river (Figure 10), that is the main supply of wash load as can be seen in Table 2 Annual suspended loads characterizing Paranà in the period 1995-2005 (Amsler et al., 2005).

The 1D advection/diffusion equation available in the model is here used to propagate fine sediment discharge, by:

$$\frac{\partial c}{\partial t} = D_{xx}\frac{\partial^2 c}{\partial x^2} + u_x\frac{\partial c}{\partial x} + kc \qquad [4]$$

with c (g/m^3) the fine sediment concentration, u_x (m/s) the longitudinal velocity, D_{xx} (m^5/g/s) the diffusivity and k sediment decay rate (s^{-1}). The diffusivity coefficient is reasonably assumed equal to the longitudinal eddy viscosity E_{xx}, calculated after Smagorinsky formula

$$E_{xx} = c_s \Delta x\left(\frac{\partial^2 u_x}{\partial x^2}\right) \qquad [5]$$

where c_s is an empirical coefficient set equal to 0.5.

The k coefficient is calibrated for each flood period of the simulated year, therefore supposing that the deposition of the fine sediments along the floodplains mainly occurs during floods.

The concentrations measured at Santa Fe-Tunel section are used to calibrate the decay rate k and to estimate sediment delay ratio as a function of river discharge for the period 1995-2007.

Firstly, the numerical simulation with annual mean discharge of the period 2002-2004 for a steady state is performed with a null sediment decay: the resulted time lag between the concentration at Corrientes and Tunel is equal to 11 days, in pretty good agreement with the estimation (9.5 days) by Re et al. (2009).

A steady hydraulic simulation is performed for each year: the mean liquid discharge of the annual flood period is imposed as boundary condition at Corrientes, while the correspondent concentration hydrogram coming from Bermejo is accounted as boundary condition at Corrientes.

The floodplain sedimentation was observed to be related to lateral discharges (Asselman & Wijngaarden, 2002; Nicholas et al., 2006) over the floodplain and the consequent flooded area. Therefore the k value is calibrated over discharge in order to reproduce the measured wash load at the Paranà-Santa Fe Tunel cross-section. The comparison between the measured and the computed concentration during floods is reported in

Table 3, showing a pretty good agreement. Table 5 shows the results of the model calibration in terms of k values.

Table 3 Concentration during floods at the Paranà-Santa Fe Tunel cross-section: comparison between data and simulations.

Year	Concentration (mg/l)	
	Measured	Computed
1994	200.5750	262.9976
1995	194.6364	286.7867
1996	242.9100	273.3380
1997	261.6250	306.1596
1998	171.7000	288.1531
1999	-	-
2000	371.4333	385.2769
2001	257.6800	292.3530
2002	333.1000	346.7855
2003	322.9556	318.1257
2004	301.1375	257.7175

Table 5 Annual suspended load and k values from validated simulations.

Year	$Q_{av,flood}$ (mc/s)	Q_{sol} (mil ton/y)		k (d^{-1})
		Bermejo	Tunel	
1995	24000	133.40	70.57	0.12
1996	18500	127.05	59.07	0.08
1997	23000	153.01	72.12	0.085
1998	32000	128.24	59.33	0.13
1999	-	-	-	-
2000	13500	102.03	47.58	0.095
2002	18500	199.99	93.49	0.065
2003	21000	205.06	94.98	0.07
2004	15700	158.04	73.94	0.03
Average	**20500**	**170.00**	**82.00**	**0.07**

The last 2 years of the studied period (2006 and 2007) are characterized by a model substantial overestimation (around 200 mg/l) of the concentrations in comparison with the observations. Concluding, the average rate of wash load depositing during floods in the period 1993-2007 between the Corrientes and Tunel sections (850 km long) is equal to 4.5 million ton per year representing the 5% of the total sediment yield (i.e., wash load from Bermejo) that incomes in the Paranà river.

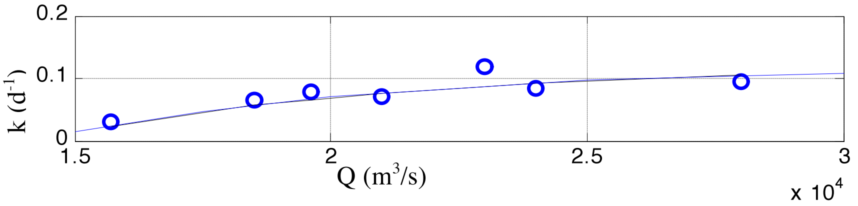

Figure 11 Liquid discharge-sediment decay rate, k, correlation (dots for simulations and solid line for interpolation).

Figure 11 Liquid discharge-sediment decay rate, k, correlation (dots for simulations and solid line for interpolation).finally shows the assessed relation between calibrated decay rate, k, and the yearly flood discharge (i.e., greater than the full bank discharge): dots represent the simulation results, while the solid line is their interpolation. The dependence law between k and Q results as exponential:

$k(Q) = a\exp(Q/b)$ [6]

with a (t^{-1}) and b (m^3/s) are equal to 0.125 and 5000 respectively.

Morphodynamic simulation

The already calibrated 1D model is applied to simulate the humid period (Figure 12) occurring within the years 1970-2000 in terms of river channel bed sediment transport, therefore calibrating the Engelund-Hansen formula for total load (i.e. bed plus suspended load from the bed) over known data of solid discharges and slope of bed and water.

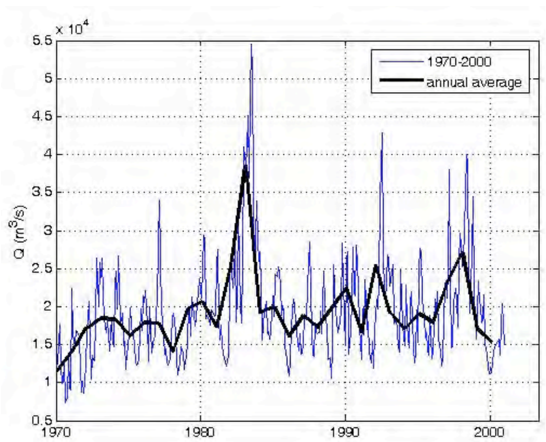

Figure 12 Discharges at Corrientes for the simulated humid period.

In order to calibrate the sediment transport formula and therefore validate the 1D model against known data along the river, three Paranà reaches are studied in more details, focusing in middle and lower part of the river: Villa Urquiza-Paranà city (10 km long) and Diamante-San Martin (85 km long) reaches for Middle Paranà; San Martin-Rosario (30 km long) reach for Lower Paranà.

The global tendencies of Middle and Lower Paranà are presented in Amsler et al. (2005) and Castro et al. (2007) respectively; the 1D model is calibrated on those morphological tendencies and on herein reported data concerning effective discharge and water slope.

The effective discharge Q_{eff} is the liquid discharge realizing the maximum sediment transport that is calculated by the product of the interval frequencies fr and the solid discharges occurring in the interval as assessed for the corresponding hydrology condition. Aiming to assess the effective discharge the Schaffernak approach to 1D model resulting data is applied. The authors divide the time series of the liquid discharge Q available at Corrientes in the XX century into constant discrete intervals of 3500 m^3/s starting from 8000 m^3/s. The choice of the these intervals is made under Biedenharn et al. (1999) and is consequent to a trial analysis of the frequency distribution of the liquid and solid discharges in order to obtain a relatively continuous histogram (as reported in Figure 13).

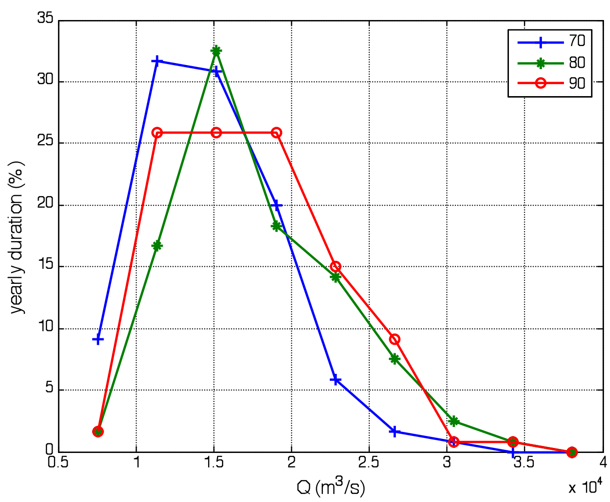

Figure 13. Yearly averaged frequency for the liquid discharge Q at Corrientes in the period 1970-90.

The effective discharge over the 1000 km long reach between Diamante and Rosario is assessed for the 3 decades of the simulation period. The results in terms of water-sediment discharge relations are shown in Figure 14, where the peaks clearly locate the effective discharge Q_{eff} on the vertical axis.

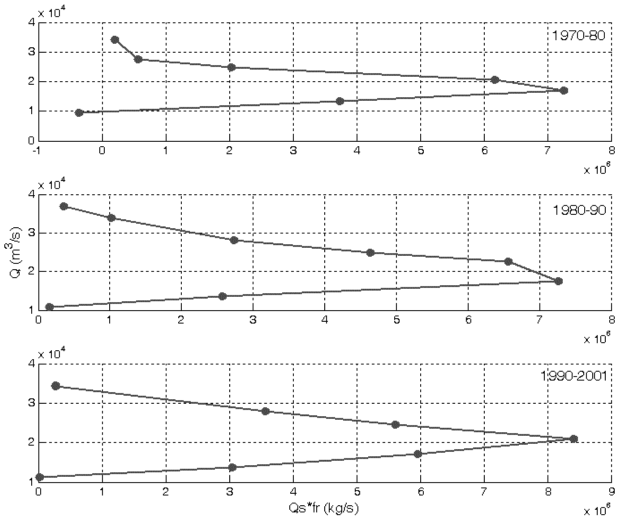

Figure 14 Period 1970-2000: effective discharge Q_{eff} for the 3 decades for the reach between Diamante and Rosario.

The 1D model values in terms of effective discharges Q_{eff}, free surface slope i_{fs} difference between Middle and Lower Paranà and sediments transport G_s are adjusted over the corresponding literature data (Castro et al., 2007) by means of the Engelund and Hansen formulation calibration; a good agreements is achieved as shown in Table 6.

Table 6 Paranà branch Diamante-Rosario in the period 1970-2000: effective discharge Q_{eff}, free surface slope i_{fs} and sediment transport G_s.

	Q_{eff} (m^3/s)		Free Surface slope difference (%)		G_s ($x10^6$ ton /y)	
	Computed	**Literature**	**Computed**	**Literature**	**Computed**	**Literature**
1970-1979	16700	17500	10	6	49	41
1980-1989	20500	20500	16.8	7.6	75	85
1990-2001	20200	20400	19	9.9	58	63

The major difference between computed and literature data is observed in terms of difference in free surface slope between Diamante-San Martin and San Martin-Rosario reaches, notwithstanding in both cases the slopes difference is positive correlated with discharge.

After the calibration, the model is validate using the data available in the Paranà city-Santa Fe Tunel cross-section for the period 1976-1998 and reported in Amsler et al. (2005). Table 7 shows the comparison in terms of effective and solid discharges, revealing a pretty good agreement.

Table 7 Middle Paranà (Tunel section) in the period 1976-1998: effective discharge Q_{eff} and sediment transport G_s.

	Q_{eff} * (m^3/s)		G_s ($x10^6$ ton /y)	
	Computed	**Literature**	**Computed**	**Literature**
1976-1980 (1970-80)*	15000	15100	23	22
1981-1990	17000	16500	32	28
1991-1998 (1991-95)*	16800	16300	28	23
Average (1976-1998)	-	-	30	25
1978 (min)	-	-	16	17
1983 (max)	-	-	70	58

The calibrated model was then applied to simulate the dry period 1950-1980 (Figure 15): the results are shown in the following figures and tables, with also some comparisons with literature data, and are used to obtain the boundary conditions for the 2D numerical model, in terms of effective discharges (Figure 16).

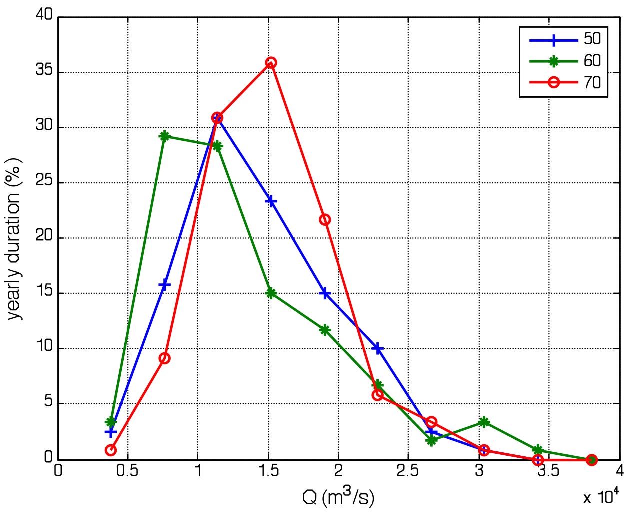

Figure 15 Period 1950-80: yearly discharge and duration.

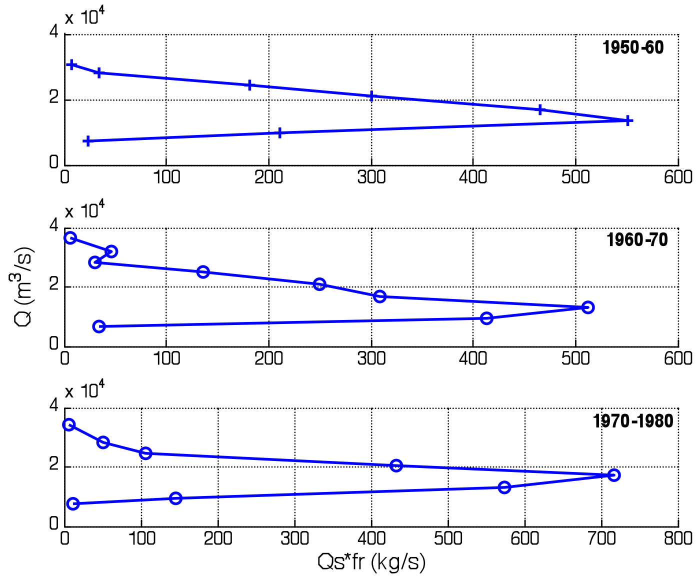

Figure 16 Period 1950-80: effective discharge Q_{eff} for the 3 decades for the reach between Diamante and Rosario.

Along the whole simulated river, two different regions can be defined with a transition around 150-200 km from downstream boundary as shown in Figure 17: within the period 1970-2000, the upstream part, i.e. the Middle Paranà, is characterized by sediment erosion and the downstream part, i.e. the Lower Paranà, with a lower channel slope, is characterized by sediment deposition. Figure 17 shows the cumulated variation of the bed elevation during simulated humid period (i.e., 1970-2000). During the humid cycle of the XX century, Middle Paranà, starting from 150-200 km upstream of Villa Constitucion (i.e., nearby Diamante), is subjected to bed erosion. Lower Paranà, instead, is characterized by an accretion tendency, since its bed elevation increases.

For the two periods, the channel bed slope change in time are reported in Figure 18 (1970-2000) and in Figure 19 (1950-80): the two regions present bed slope increase until 1970, after which, with discharge increasing, the bed slope at Lower Paranà decrease that correspond to bed accretion. These results are in accordance with the study carried out by Castro et al. (2007), based on measurements in few sections. The 1D model simulations confirm two different regions along Paranà, characterized by different water discharge-bed slope correlations.

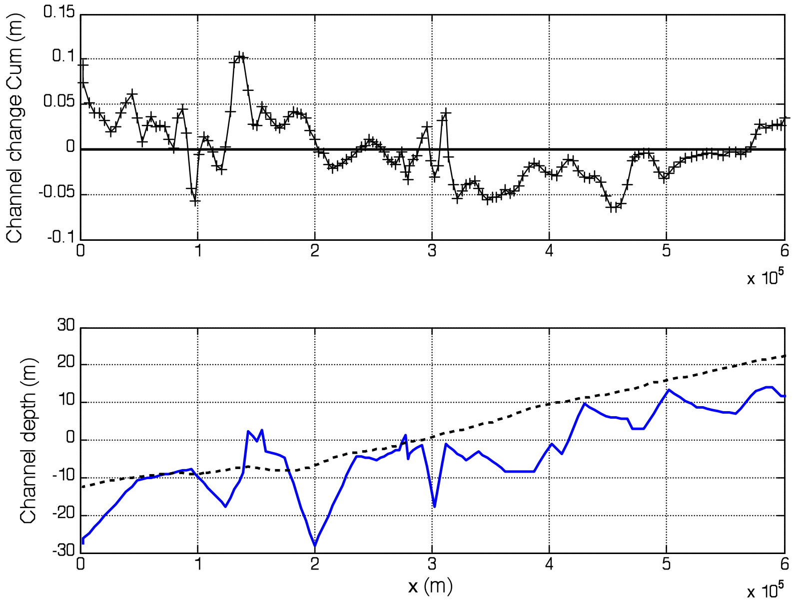

Figure 17 Humid period 1970-2000. Cumulated channel change and longitudinal profile for the simulated Paranà reach.

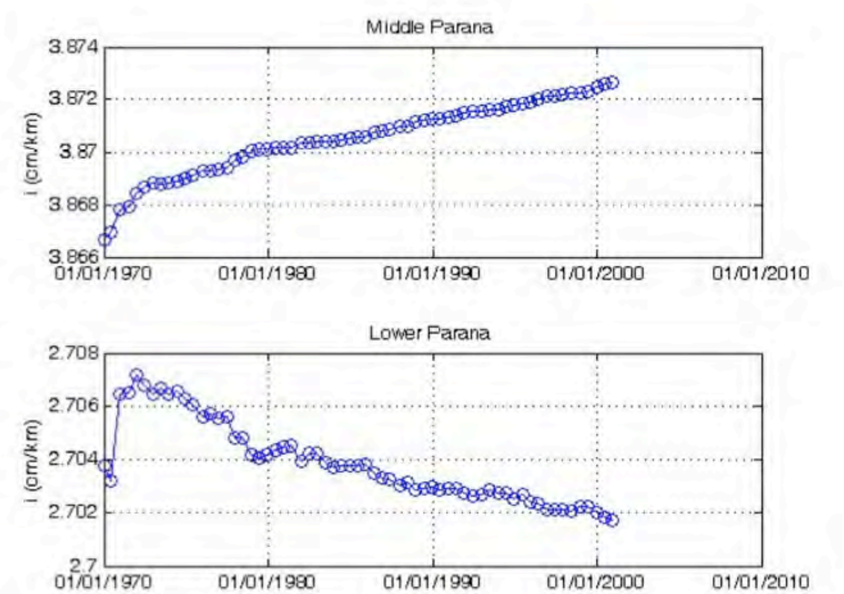

Figure 18 Humid period 1970-2000. Channel slope evolution in Middle and Lower Paranà.

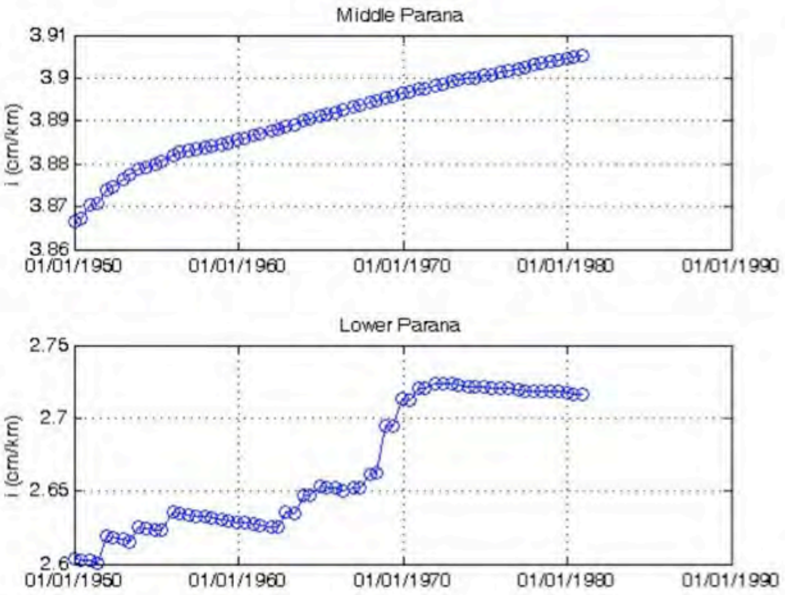

Figure 19 Dry period 1950-80. Channel slope evolution in Middle and Lower Paranà.

The calibrated model finally provides the upstream boundary conditions for the 2D numerical model in terms of:

- effective discharge Q_{eff} and its duration d for each 10 years within the study period (1954-1976) reported in Figure 20, evaluated as the equivalent value that is able to produce the 80% of the total sediment volume transported at Rosario cross-section;

- correspondent solid discharges Q_s (80% of the total sediment volume) in Table 8.

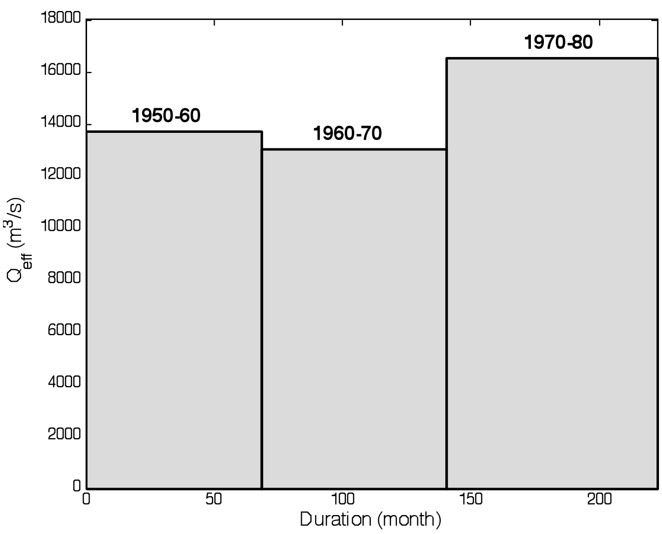

Figure 20 Effective discharge and duration for boundary conditions of 2D numerical model (Carlota island reach).

Table 8 Hydraulic and sediment data for 2D model boundary conditions (Carlota island reach), h_{eff} are at downstream boundary (Rosario-Victoria Bridge) of the 2D model.

	Q_{av} (m^3/s)	Q_{eff} (m^3/s)	h_{eff} (m)	d (month)	G_s (mil ton /y)
1950-1959	16200	13700	4.4	68	39
1960-1969	15200	13000	4.1	72	38
1970-1980	16900	16500	5.8	83	45

Lower Paranà case study

The 24 km long reach of Lower Paranà (Figure 21) was surveyed during three field campaigns in June 2009, August 2009 and November 2010, using a single beam ecosounder, three acoustic current Doppler profiler (hereafter ADCP), a water-suspended sediment sampler; all the instruments were real-time referenced with a RTK-GPS. The first campaign accomplished to survey the current bathymetry for 2D model implementation and the velocity field at 8 cross-sections and along the thalweg. The following two campaigns were mainly devoted to sediment transport. In the present document, we present only the results of first survey, also used to calibrate sediment transport formula in the 2D model, while the 2010 campaign data are under processing.

The validation of the 2D numerical model MIKE21C by DHI is performed in 3 distinct phases: the bed roughness is calibrated within the shallow-water approach of the model, by the comparison of measured and computed depth maps and velocity vectors at surveyed cross-sections; then the sediment transport formula of Engelund and Hansen is adjusted on measured concentration; finally, the long term morphodynamic simulations are carried out in order to reproduce the island Carlota formation process occurring in the period 1954-1976 accounting of hydrodynamic and sediment transport former calibration results and of the historical cartography.

The sensitivity analysis results bears out helical flow and transversal slope effectiveness on sediment transport and on the consequent developments of island Carlota and the related upstream bifurcation.

Figure 21 The case study for Lower Paranà.

Field surveys

The performed campaigns are aimed to investigate: 1) the velocity field, 2) bed forms and their effect on hydraulic roughness, 3) the channel bathymetry, 4) and sediment transport.

Velocity field investigation

The first campaign was carried out in 29 June - 3 July 2009. The velocity field was investigated at 8 cross sections and along the longitudinal track following the channel thalweg (Figure 22).

In order to increase the reliability of collected data, 2 ADCPs were simultaneously deployed from a boat moving across the river to measure the same discharge: the 600 kHz ADCP by Teledyne RDI and the 1000 kHz ADCP by Sontek: the former was relative referenced across the river with the acoustic signal devoted to track the bottom (i. e., Bottom Track or BT signal, see RDI Instruments 1999), the latter was absolute referenced with a RTK-GPS.

The depth was measured with the single beam echosounder by Raytheon integrated to Sontek ADCP acquisition. The compass of the ADCPs was in field calibrated.

Each cross-section was measured at least 2 consecutive times, the following table reassumes the survey results in terms of total measured discharge and length at each cross-section; it also reports the number of repeated transects at each track.

Table 9 Comparison of resulting discharges of June-July 2009 campaign among different instruments and sub-reaches.

River cross-section	1000 kHz ADCP by Sontek (DGPS-RTK referenced)			600 kHz ADCP by Teledyne RDI (BT referenced)		
	Discharge [m^3/s]	Length [m]	Measured transects	Discharge [m^3/s]	Length [m]	Measured transects
1	13786	1113	2	13996	1139	2
2	10508	790	2	11336	816	2
3	2755	687	2	2755	699	1
4	721	217	2	821	223	2
5	13271	674	3	12893	708	1
6	4131	562	4	4216	583	3
7	9324	902	3	9749	907	2
8	13741	1853	3	13901	1839	2

The total river discharge can be evaluated by summing bifurcated reaches contribute (2 plus 3, 4 plus 5, 6 plus 7 cross-sections) or simply considering cross-section 1 or 8, the obtained 5 assessments results on average equal to 13647 and 13933 m^3/s for Sontek and RDI ADCP respectively. Sontek ADCP estimation is more accurate thanks to the adopted methods for instrument position (DGPS-RTK) and water depth (echosounder) measurements, notwithstanding the RDI value is only 2% higher that bears out the absence of significant systematic errors during the campaigns.

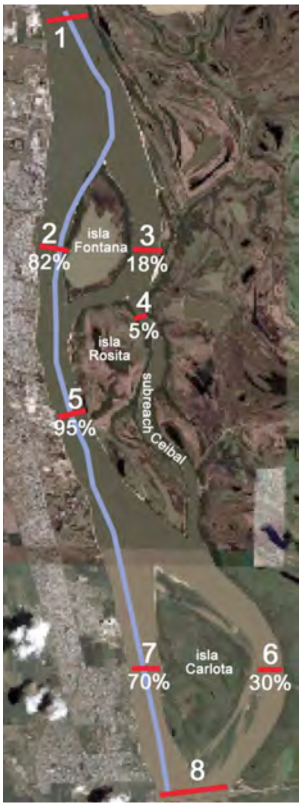

Figure 22 ADCP transects and discharge repartition (June-July 2009 campaign).

Figure 22 shows the resulting (Sontek ADCP data) discharge repartition between bifurcated reaches.

During the campaign, the water level, continuously acquired by the Prefectura Naval, was 5.2 m s.w.l. at Rosario, that is 17 km downstream from section 8, and 6.1 m s.w.l. at S. Martin, that is 31 km upstream from Rosario. The resulting water slope during the campaign is 2.7 cm/km.

Bed forms investigation

The velocity field and the bed profile along the longitudinal track are analyzed aiming to characterize the alluvial roughness along thalweg, since the measured velocity profiles and depth give evidences on dune morphology. Figure 23 reports the ADCP measured velocity field within the first kilometer of the longitudinal track and the corresponding depth signal, showing the classical dune stoss (gently sloped and "windward")-lee (steep) sides morphology of dune and the related acceleration-deceleration across the dune crest-trough profile.

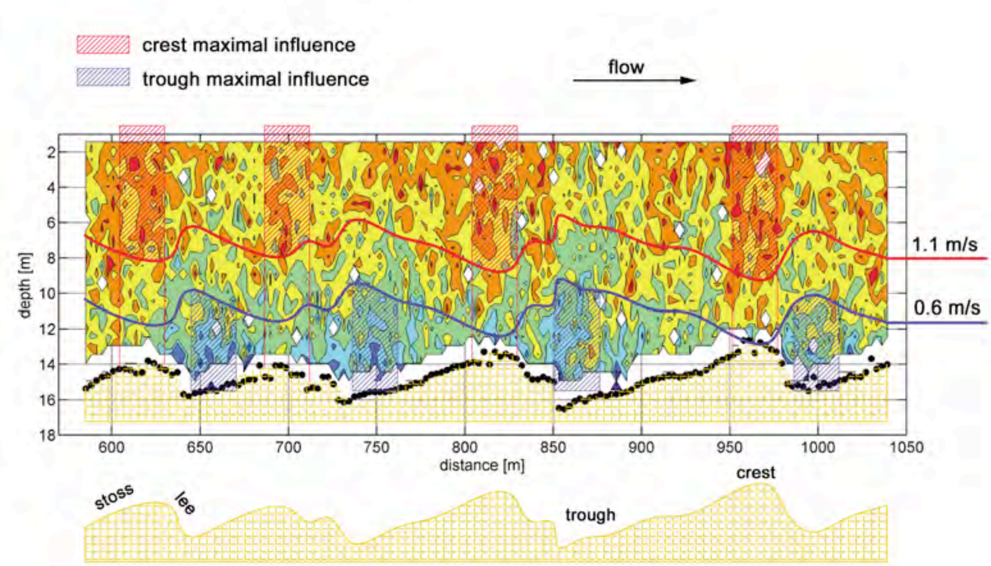

Figure 23 Velocity magnitude along dunes from ADCP longitudinal transects (June-July 2009 campaign).

By extending the dune analysis to the longitudinal whole track, we investigated the alluvial roughness variation along thalweg. In particular we found that dune steepness increase with depth.

Alluvial roughness is proportional to dune steepness (Yalin & da Silva, 2001) that is defined as dune amplitude to length ratio. Beside dune morphology features (i.e. wave amplitude and length), roughness could also be inferred by evidences regarding the generated shear stress. In particular, under Guerrero & Lamberti, friction velocity is assessed using velocity and "error velocity" profile (RDI Instruments, 1999), measured with ADCP.

The whole track is divided in 5 equal segment aiming to separate large scale morphology features (i.e., bifurcation, junction, ecc.) as can be seen in Figure 24.

Figure 24 Sub-reaches for bed forms analysis.

The average wave length and amplitude are evaluated by means of spectral analysis of depth signal carried out at the 5 not-overlapping sub-reaches. The resulting values are correlated to corresponding mean depths (Figure 25): the correlation between depth and dune steepness at large scale morphology is equal to 0.8.

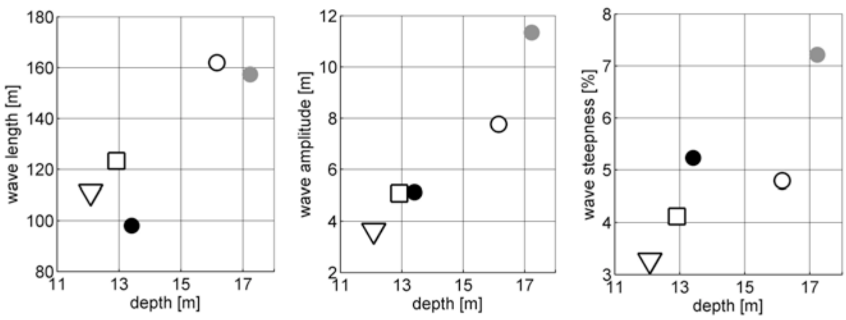

Figure 25 Resulting dune wave amplitude and length at different depths.

Figure 26 reports the analyzed depth signal and the depth averaged velocity as resulting from ADCP profiles and also shows the 5 sub-reach edges. ADCP data bear out positive correlations of 0.5 and 0.6 between depth and depth averaged velocity, and between depth and shear stress respectively at large scale morphology.

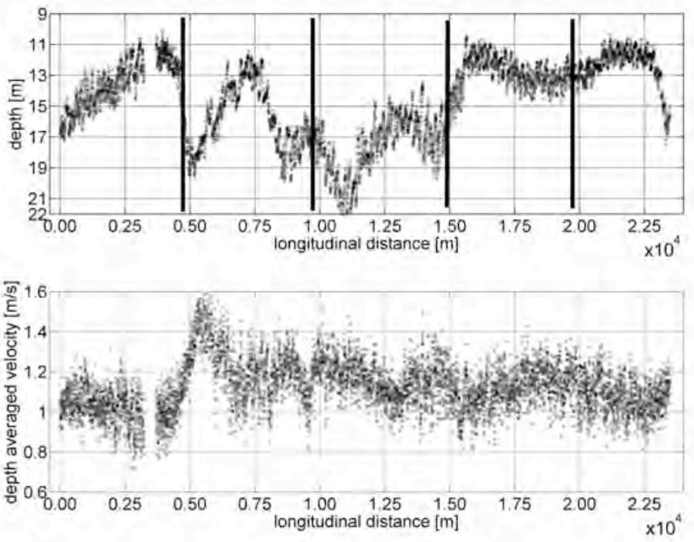

Figure 26 Depth and depth averaged velocity along thalweg (June-July 2009 campaign).

Bathymetry investigation

The 2009 June-July campaign was also aimed to survey current bathymetry to be compared to historical maps and to be applied for 2D numerical simulations. The echosunder was deployed across the river following near to 200-300 meters separated cross-sections (Figure 27) therefore measuring water depth.

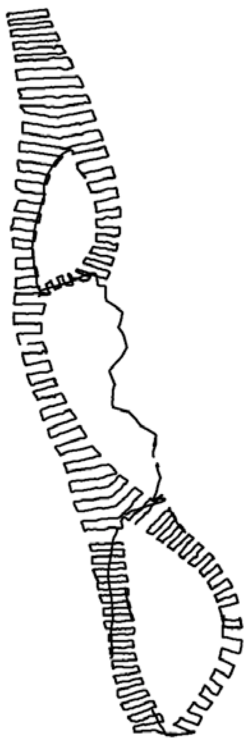

Figure 27 Echosounder track (June-July 2009 campaign).

The measured data are then transformed in bed levels accounting of Prefectura Naval data during the campaign, in particular: 1) the water surface level at Rosario, 2) the water slope between Rosario and S. Martin, 3) the distance of each cross-section to Rosario water stage. Further recent topographic data of island and margin were finally integrated on the 50x50 mesh before the Kriging interpolation, therefore achieving the river reach complete bathymetry.

Sediment transport investigation

The second campaign was aimed to characterize incoming sediment transport at case study reach. The studied sections herein are located near the city of San Martín. The sections were arranged upstream of the upstream large, asymmetrical, bar-bifurcation. The measurements were perfermed from 12 to 13 August, 2009. The total measured flow discharge was approximately 16700 m^3/s, the water level at Rosario around to 6.4 m s.w.l and the water slope 2.9 cm/km as inferred from S. Martin-Rosario water level increment (Prefectura Naval data). The three-dimensional flow velocity field and backscatter were measured with a 1000 kHz Sontek and 600 and 1200 kHz Teledyne RDI ADCPs at sections SM1 to SM4 (Figure 28).

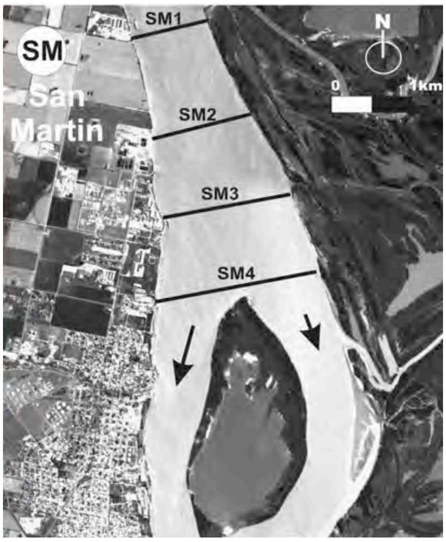

Figure 28 ADCP transects (August 2009 campaign).

Two Teledyne RDI ADCPs, working at different frequencies (600 and 1200 kHz), were used simultaneously on the same water column to investigate the suspended sediment concentration and grain size distribution by means of sound backscatters (Guerrero et al., 2011). In the same campaign, the echo measured by a Sontek 1000 kHz ADCP previously calibrated against the sand content of water samples was also used (Szupiany et al., 2007). The wash load (silt and clay) was neglect because it plays a marginal role in the morphodynamic processes operating within the main channel of the Paraná River, notwithstanding it represents the 80% of the total amount of sediment transport that was estimated around 130-135 10^6 t/year on average in the period 1976-1998 at Tùnel Subfluvial cross-section, Lower Paranà at Paranà-Santa Fe, as reported by Amsler et al. (2005). The same authors also report that about the 90% of river bed sediments (around 25 10^6 t/year) are transported as suspended load and the rest as bed load. Therefore is widely accepted that suspended sediment plays the most important role in bed morphodynamics.

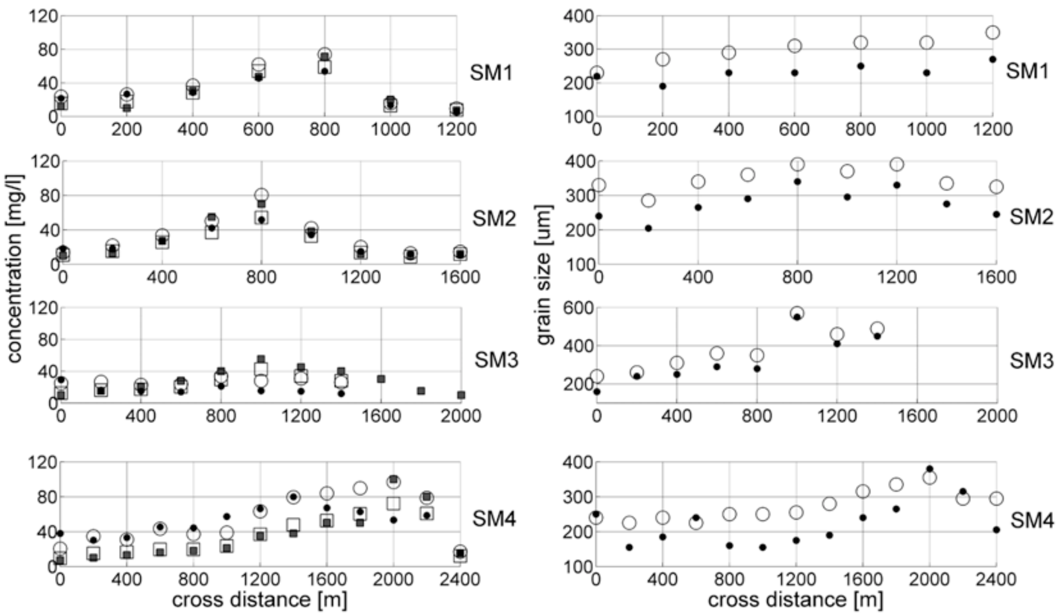

Figure 29 Comparison of the results among different instruments and methods of concentration and grain size at 4 cross-sections (gray and white squares result from one frequency methods: Sontek and 1200 kHz RDI ADCPs without sand attenuation, respectively; black and white dots result from the two frequencies, 1200/600 kHz RDI-ADCPs, method, using 200 and 300 μm, respectively, as the expected mean grain size).

Figure 29 compares depth averaged concentration and grain size of suspended sand at the 4 surveyed cross-sections among different 1) instruments, 2) applied methods to process the echoes and 3) calibrations.

Depending on the instrument setting and application the incoming mean concentration results within 30-40 mg/l, corresponding to 16-21x10^6 t/year, and the mean suspended grain size is around 300 µm.

Concentration and grain size distribution are analyzed in more details along river cross-sections to be correlated to ADCP measured velocities and depths. Firstly we looked for evidences at the whole cross-section morphology, 1-2 kilometers as length scale. As expected, depth averaged velocity is found to be positive correlated with depth. The concentration and grain size distribution are positive correlated, as can be seen in Figure 29, but negative correlated to depth. With the aim to look for short length scale correlations, longer than 200 m wave length components are filtered from analyzed signals, obtaining a filtered signals showing significant positive (i.e., 0.4) correlation between depth and concentration and negative (0.4 as magnitude) between concentration and grain size.

Therefore, two different behaviors arouse depending on morphology length scales: the most of suspended coarse sand is transported at low depth areas of cross-section channel, reflecting the primary flow variability along the section. Whereas, a relative high concentration of relative fine sand is observed at highest filtered depths, understanding that as the superimposed effect of dune morphology (i.e. short length scale effect).

2D numerical simulations

The 2D code MIKE21C by Danish Hydraulic Institute using shallow water approximation is used to simulate the 24 km long surveyed reach. The model solves in two dimensions 1) the equations of Navier-Stokes for water motion, 2) the equation for suspended sediments convection-diffusion and 3) the Exner equation for bed morphology development, on a curvilinear grid using the finite difference scheme. A wet and dry algorithm allows water stage to change significantly during simulation, except near the boundaries. Bed roughness can be defined as a constant, as a map or variable with depth in order to account of bed forms shear. Sediment transport generation can be eventually subdivided between bed- and suspended-load by applying and also calibrating many author formulations.

Hydrodynamics vertical dimension features, i.e. logarithmic profiles and helical flow, are taken into account both on the two-dimensional convective-diffusive equation and on bed load. The 2D convective-diffusive equation is derived from the Galappatti (1983) approach for quasi steady concentration profile, and assuming the equilibrium of concentration near the bed. In that way the concentration time and spatial derivatives are multiplied by coefficients coming from velocity and concentration profile vertical integrations, but that can be also tuned in agreement with field evidences. The bed load is diverted from velocity direction depending on bed slope and channel curvature as described by first order model of Kalkwijk & Booij (1986) that can be calibrated in agreement with field evidences. These features make the model quasi 3D, but introduce some parameters that need to be accurately calibrated.

In agreement with mentioned schemes, the sediment continuity and convective-diffusive equations are solved in a quasi steady approach also with the aim to speed up long term morphodynamic simulations. For this reason, the model is particularly suitable for long term and slowly variable morphodynamics simulations.

Later erosion/deposition is simulated nearby banks (i.e. grid boundaries) or within the model area, the latter option aims to represent islands formation process. In particular, lateral erosion/deposition can be calibrated by adjusting its proportionality to sediment load of adjacent cell and/or to transversal slope of the bed (i.e. near margin slope).

Three simulations are performed, with a specific objective: 1) the hydraulic simulation of the whole 24 km long surveyed reach on the hydrological steady condition of July 2009 campaign is aimed to accurately calibrate the hydraulic roughness to be used in the following simulations; 2) the same 24 km long reach is then simulated on the hydrological steady condition of August 2009 in order to calibrate the applied Engelund & Hansen (1967) formulation for sediment transport to be used in the following simulation; 3) finally, the long term morphodynamic simulation is carried out on the 11 km long downstream subreach including the island Carlota (cross-sections 9 to 14 in Figure 2) and within a significant period, 1954-1976, for island formation, aiming to calibrate transversal slope/helical flow effects on sediment transport and consequently on lateral process affecting bifurcations dynamics at Lower Paranà.

Hydrodynamics calibration

The calibration of Paranà hydrodynamics is carried out on the steady condition that were surveyed on July 2009 campaign, in particular ADCP measured discharge and water stages data at San Martin and Rosario are assumed to infer boundary conditions and, as already mentioned, to reference the echosounder measured bathymetry. The curvilinear grid is tailored on the measured bathymetry also accounting of recent topographic data regarding margins and islands and, at this stage, neglecting the Ceibal secondary reach because it only conveys the 5% of the measured discharge (Figure 22). Longitudinal and transversal length of grid cells are 220 m and 70 m respectively on average, as result from the applied compromise between simulation accuracy/resolution and computational resource consuming for following long term morphodynamic simulations that use the same grid spacing.

Figure 30 shows the 110x39 cells of the computational grid and the corresponding 2009 bathymetry.

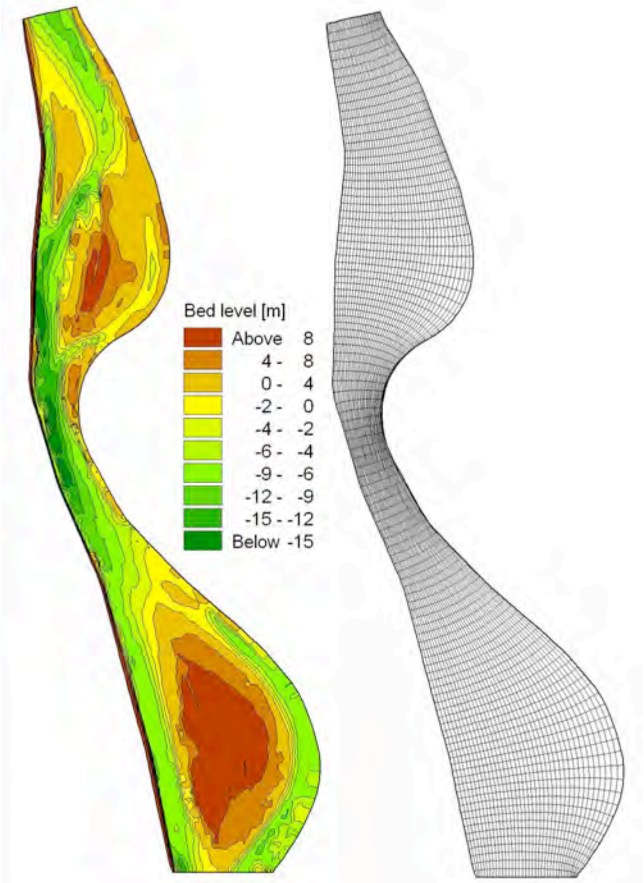

Figure 30 Bathymetry from June-July 2009 campaign for the 2D model and its computational grid.

Upstream boundary condition is the measured discharge of 13650 m^3/s, incoming velocity vectors in the model are aligned in agreement with ADCP measured and depth averaged vectors. Downstream boundary condition is 5.6 m s.w.l. as it results by adding the measured water stage level at Rosario, 5.2 m s.w.l., to the Rosario-model boundary (i.e. Rosario-Victoria bridge) increment of water level, 0.4 m, with respect to the, inferred from water stages, mean slope, 2.7 cm/km, between S. Martin and Rosario. The applied boundary condition of 5.6 m s.w.l is about 1 meter higher than water level corresponding to measured discharge of 13650 m^3/s as would results from 1D simulated water stage-discharge relation, that actually is a steady conditions relation not accounting of observed level deviations during rising and falling phases of water stage. These deviations resulted from 1D model to be on average within a 2 meter interval centered with respect to the mean steady relation, that is in agreement with 5.6 m s.w.l. as inferred from water stage data measured within June-August 2009 corresponding to a mean rising of 1.6 cm/day.

Simulations results are compared to ADCP and bathymetric survey of June-July 2009 campaign, aiming to calibrate hydraulic roughness by means of Gauckler-Strickler parameter. In particular simulated depth are compared to echosounder depth along the whole domain, velocity vectors are compared at ADCP measured cross-sections, except 1, 8 that are nearby the model boundaries, the velocity magnitude measured along thalweg is compared to simulation results at the same track. Figure 31 and Figure 32 show the best agreements achieved using 45 $m^{1/3}s^{-1}$ as Gauckler-Strickler parameter, in that case the depth deviation are lower than 4% on average, and the mean deviation of velocity magnitude along thalweg is near to 8%.

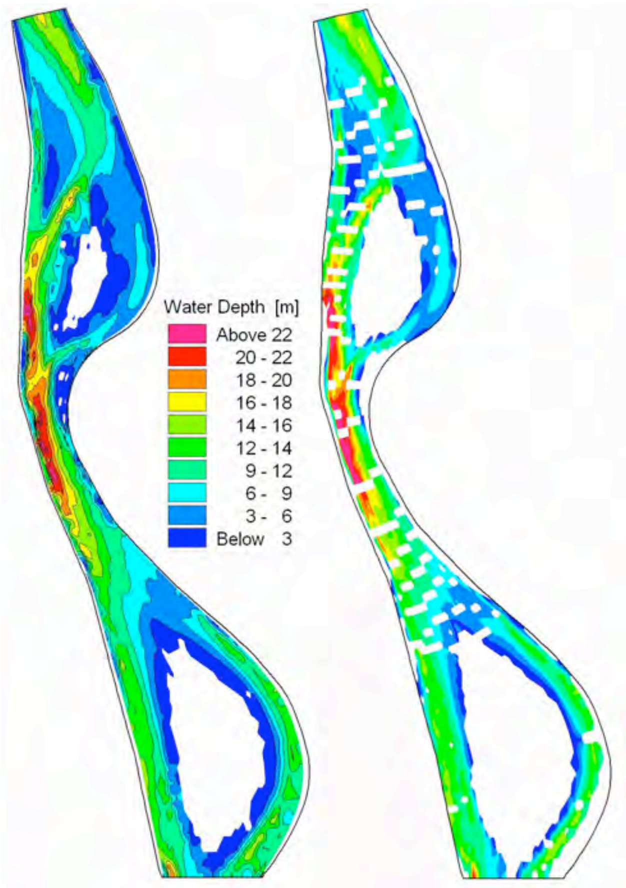

Figure 31 2D simulated (left) and measured (right) depths.

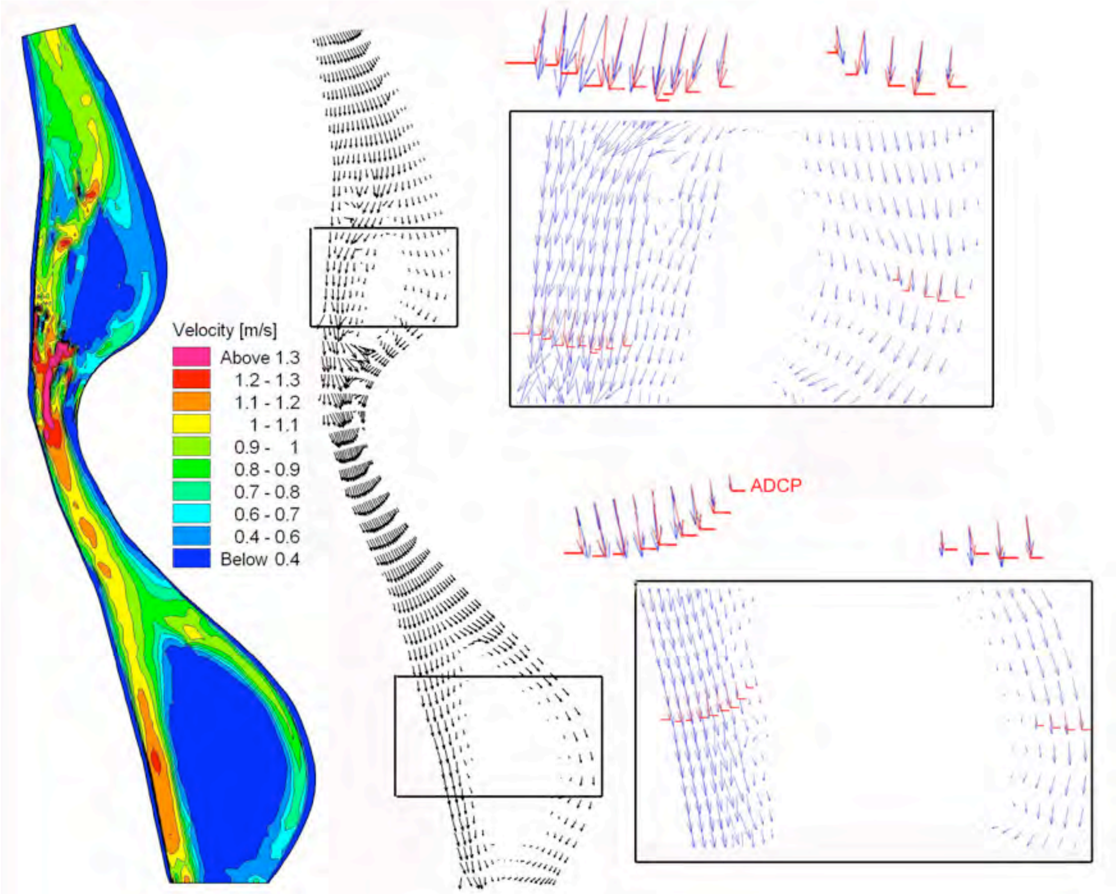

Figure 32 2D simulated velocity field and velocity vectors comparison to ADCP measurement at sub-reaches.

Sediment transport calibration

The calibration of sediment transport formula is carried out on the steady conditions of August 2009 applied to the same domain and bathymetry used for the hydraulic calibration. The upstream boundary condition is 16700 m^3/s, meanwhile the downstream boundary level is 6.8 as resulting from Rosario water stage of 6.4 m s.w.l. and from inferred water slope of 2.9 cm/km.

The steady depth-averaged concentration field of single size material is simulated, representing the river bed mean sand (0.3 mm), by means of a single infinite thickness layer. Wash load is neglected since it plays a marginal role within river channel morphodynamics. Total sand transport is subdivided into 10% of bed- and 90% of suspended-load in agreement with data from literature.

The obtained suspended concentration is compared to ADCP inferred depth averaged concentrations in Figure 33. The ADCP data only accounts of suspended sand because of the insensitivity of the used frequencies to clay and silt (wash load) and because of the acoustic shadow near the bed (bed load).

The good agreement between ADCP measured and simulated concentrations is accomplished by the calibration of applied sediment transport formula for suspended load in the model. In particular we applied the Engelund & Hansen formula that is a total load formula therefore, concerning suspended load, it is reduced to 90%, the rest is simulated as bed load. Furthermore the Engelund & Hansen formula used in the model is multiplied by the calibration parameter resulted equal to 2. Notwithstanding that Engelund & Hansen formula is indicated in literature (Alarcon et al 2004, Amsler et al. 2005) as the best fitting for Lower Paranà sediment transport historical data, the pretty high calibration parameter accounts of the applied hydraulic roughness, 45 $m^{1/3}/s$ as Gauckler-Strickler parameter. That value introduces in the model higher shear stress, accounting of alluvial roughness, in comparison with the skin friction corresponding to 0.3 mm as grain size that is usually applied in combination with Engelund & Hansen formula.

Figure 33 Suspended concentration at investigated cross-sections.

Morphodynamics calibration

The calibration of Paranà morphodynamics is carried out at the 11 km long subreach of island Carlota that is within river cross-sections 9-14 in Figure 2. As can be seen in Figure 34, that subreach significantly changed during the XX century in a way that is representative of Lower Paranà morphodynamics. The Carlota Island was formed in the middle of the active part of the river as the consequence of a deposition process that took place at Lower Paranà.

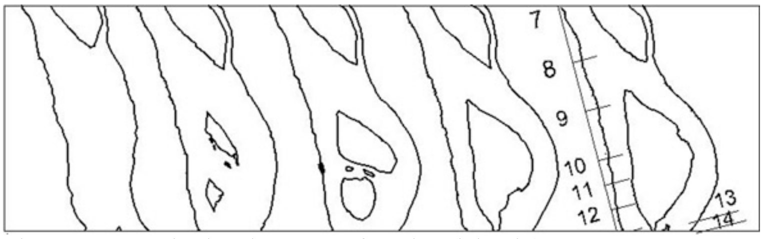

Figure 34 Margin development of Carlota island (1954-1976-1987-1993-2004 from left to right).

As a matter of fact, due to its bed slope, the sediment transport capacity of Lower Paranà is lower than Middle Paranà capacity as it arises from 1D model. The deposition at Lower Paranà occurred among the whole XX century driving river channel from intricate braided morphology to a meandered-bifurcated configuration that is characterized by the sequence of well defined islands in between a straight main channel and a secondary bended channel. That oversimplification was particularly intense during the second part of XX century, corresponding to a humid period driven by climate interdecadal oscillation (Amsler et al., 2005) that probably also intensified the unbalance between Lower and Upper Paranà sediment transport capacities. Figure 2 and Figure 34, more detailed for Carlota island, shows the margin collections from 1954 to 2004 that witnesses the described morphology change. In particular the Carlota island formation arose at cross-sections 9 to 14, between 1954-1976 period. That process was also characterized by the left margin displacement of 1.5 km within 1954-2004 and by the diversion of main flow from left bended to right straight channel. Castro et al. 2007 carried out a detailed morphology analysis of the whole reach of Figure 2, also reporting that the water volume and the averaged depth of main channel respectively changed from $9.5x10^6$ m^3/km and 5.2 m to $10.1x10^6$ m^3/km and 7.4 m within the period 1950-2005, for the 10 km that include the Carlota island. Based on historical margins in

Figure 34, the mentioned data, the averaged level resulting from 1D model we reconstructed the 1954 bathymetry starting from the survey bathymetry of 2009. The obtained depth map for 1954 is reported in Figure 35 where it can be compared with 2009 depth map. The water volume and the depth as average over the map result equal to 9.1x10^6 m^3/km and 4.6 m respectively for 1954 and 15.5x10^6 m^3/km and 8.1 m for 2009.

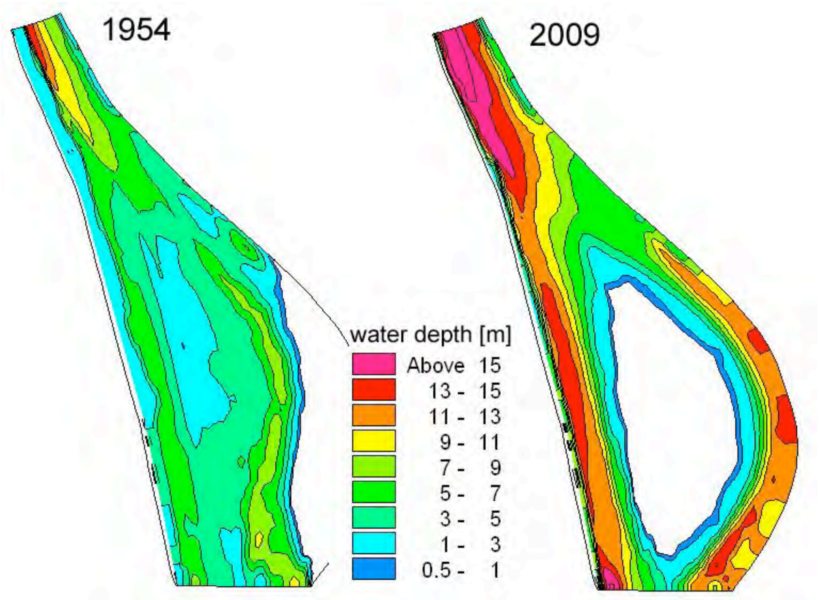

Figure 35 Reconstructed (1954) and measured (2009) depths.

The reconstructed bathymetry of 1954 is forced with steady conditions at the boundaries as resulting from 1D model within the simulation period. The quasi-steady approach was applied by simulating the three consecutive effective discharges for their durations within the periods 1954-59, 60-69 and 70-76. The used morphological time step is 12 hours accounting of expected morphodynamic rate. The computational grid is the part of entire reach model (Figure 30) that covers the downstream 11 km with 55x39 cells. Bed roughness and calibration parameters for Engelund & Hansen formulation are fixed on the hydrodynamic and sediment transport calibration results.

A sensitivity analyses is carried out on helical flow and transversal slope parameters that are accounted on the concentration profile parameterization and on bed load direction assessment. In particular MIKE21C by DHI (2002) applies the following formulation to assess bed load in the direction perpendicular to mean flow direction (i.e., transversal bed load S_n):

$$S_n = \left(tg\delta - G \cdot \theta^{0.75} \cdot \frac{\partial z}{\partial n} \right) \cdot S . \qquad [7]$$

The angle δ represent the deviation due to secondary currents and is modeled along flow direction s by means of the Equation 8 as described by Kalkwijk & Booij (1986)

$$\lambda \cdot \frac{\partial tg\delta}{\partial s} + tg\delta = -\beta \cdot \frac{h}{R} , \qquad [8]$$

where λ is a length scale related to water depth h and hydraulic roughness, R is the radius of curvature along s and β is the calibration parameter that is expressed as a function of Von Karman constant k and the dimensionless Chezy coefficient C:

$$\beta = \alpha \cdot \frac{2}{k^2} \left(1 - \frac{1}{k \cdot C} \right) . \qquad [9]$$

The negative term in Equation 7 accounts of the effect on bed load direction of bed slope in the transversal direction n, by means of the Shields coefficient θ and the calibration parameter G. The helical flow and transversal slope counteract on river channel morphology: the helicoidally secondary currents drives sediment depositions to deviate stream flow giving rise to braided morphology, meanwhile transversal slope reshapes channel cross-section because of gravity force on sliding sediments.

The sensitive analyses is aimed to calibrate the opposite contributes in Equation 7 on bed load by reproducing Carlota island formation within 1954-1976 period, the bifurcation and related bar developments being affected by lateral erosion-deposition process.

Beside transversal bed load, lateral erosion is also modeled. This process is modeled on the assumption that the shape of the transverse bed profile does not change. Therefore, from geometrical considerations the bank erosion rate is fixed to be proportional to the bed erosion. The coefficient of proportionality corresponds to the transverse bed slope that was assumed equal to 1 over 30 as average in the area.

The most significant depth map that results at the end of simulated period (i.e., 1976) can be compared to the 1976 margins in Figure 36 where the corresponding helical flow and transversal slope parameters are also reported.

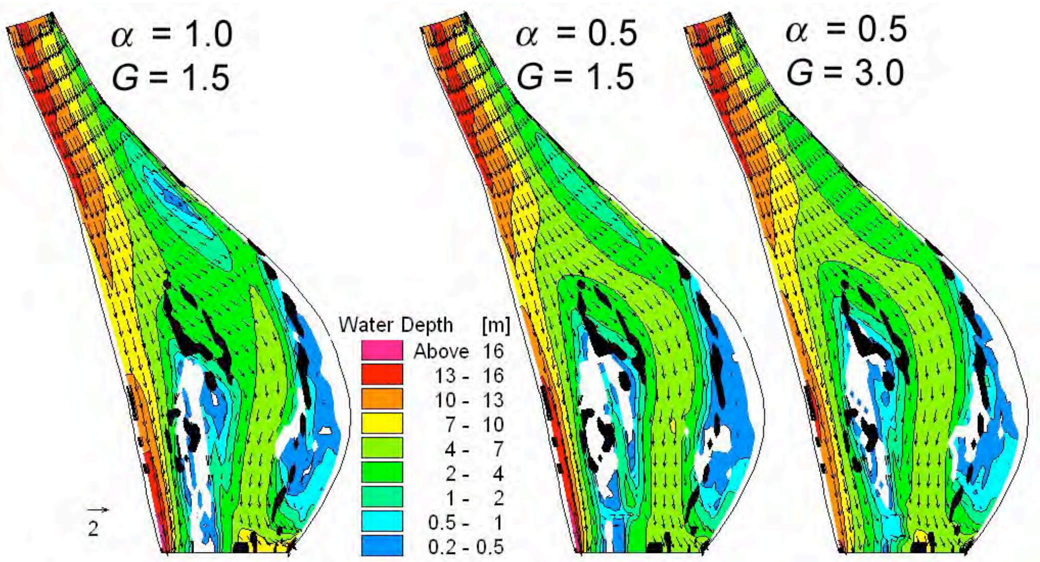

Figure 36 Comparison of 1976 historical margin to resulting depth maps from 2D model simulations of 1954-1976 period and for different helical flow (α) and transversal slope (G) parameter values.

Results

The main result within the D 9.13 deliverable, "Model of the geomorphology and sediments in the Lower Paranà River", is the calibration of a methodology useful to predict future tendency of Lower Paranà river morphology. The methodology will be applied to future climate scenarios.

In Particular we accomplished to calibrate a 1D numerical model including the Paranà-Paraguay whole system that when forced with flow discharge at its upstream boundaries is able to produce hydraulic and sediment transport condition for the detailed 2D model of Lower Paranà reach. The 1D model also represents discharge-bed slope change correlation that will be useful to predict future morphology changes at large scale. The 2D simulated reach of Lower Paranà is only 24 km long but includes two bifurcations and two junctions at the San Martin-Rosario area and therefore it significantly represents divagation of the river channel that interferes with the navigation way. The 2D model was calibrated on past climate interdecadal variability and will be used to predict future braiding-meandering tendency of the active channel of the river under different climate scenarios.

References

Alarcón, J.J., Szupiany, R., Montagnini, M.D., Gaudin, H., Prendes, H.H. & Amsler, M.L., 2003. Evaluación del transporte de sedimentos en el tramo medio del río Paraná. Nuevas tendencias en Hidráulica de Ríos, Primer Simposio Regional sobre Hidráulica de Ríos (CD ROM), Ezeiza, Buenos Aires, Argentina.

Amsler, M.L., Ramonell, C.G. y Toniolo, H., 2005. Morphologic changes in the Paraná River channel (Argentina) in the light of the climate variability during the 20th century, Geomorphology 70: 257-278.

Asselman N.E.M & M. Van Wijngaarden, 2002. Development and application of a 1D floodplain sedimentation model for the River Rhine in the Netherlans. J. Of Hydrology, 268, 127-142.

Doyle M.E., Barros V.R., 2010. "Attribution of the river flow growth in the Plata Basin", International Journal of Climatology, DOI: 10.1002/joc.2228.

Biedenharn D.S., ThorneC.R, Soar P.J., Hey R.D., Watson Ch.C., 1999. A practical guide to effective discharge calculation, US. Army Corps of Engineers.

Castro, S. L., Cafaro, E. D., Gallego, M. G., Ravelli A. M., Alarcón J. J., Ramonell, C. G. y Amsler, M. L., 2007.Evolución morfológica histórica del cauce del río Paraná en torno a Rosario (km 456 – 406), CONAGUA 2007, Argentina.

DHI Water & Environment, 2002. Mike21C River Hydrodynamics and Morphology, DHI, Horsholm, Denmark.

Engelund F., Hansen E., 1967. A monograph on sediment transport in alluvial stream. Teknisk Forlag. Danish Technological University. Copenhagen, Denmark.

Galappatti R., 1983. A depth-integrated model for suspended transport. Communications on Hydraulics 83-7. Dept. of Civil Engineering, Delft Univ. of Technology.

Garcia N.O. and W.M. Vargas, 1998. The temporal climatic variability of runoff and precipitation in the Rio de la Plata basin. Hydrological Sciences Journal, 41 (3), 279-299.

Garcia N.O., Vargas W. M., Venencio M., 2002. About of the 1970/71 climatic jump on the Rio de la Plata basin. Proceedings 16th Conference on Hydrology. American Meteorological Society, pp. 138-141.

Guerrero M., Lamberti A. Flow field and morphology mapping using ADCP and multibeam techniques: a survey in the Po River. Under review.

Guerrero, M., Szupiany, R.N., Amsler, M., 2011. Comparison of acoustic backscattering techniques for suspended sediments investigation, II Symposium on Experimental Methods in Hydraulics (MEH 2011), Bahía Blanca, Argentina, 28-31 March 2011.

Kalkwijk J.P.T., Booij R., 1986. Adaptation of secondary flow to nearly horizontal flow. Journal of Hydraulic Research, 24(1), 19-37.

Maciel, F., Díaz, A., Terra, R., 2010. "Variabilidad multi-anual de caudales en ríos de La Cuenca del Plata", IAHR-AIIH, XXIV Congreso Latino Americano de hidráulica, Punta del Este, Uruguay, November 2010.

Nichols, A.P., Walling D.E., Sweer R.J, Fang X., 2006. Development and evaluation of a new catchment-scale model of floodplain sedimentation. Water Resources Research, 42, W10426.

Re M., Menendez A., Amsel M., 2009 : Metodologia para la generacion de series temporales de descarga solida de los rios Paranà de las Palmas y Paranà Guazù. RIOS 2009.

RD Instruments, 1999. Acoustic Doppler Current Profiler, Principles of Operation A Practical Primer. San Diego, CA, USA.

Saurral, R., 2010. The hydrologic cycle of the La Plata Basin in the WCRP-CMIP3 multi-model dataset. J. Hydrometeor., 11 (5).

Szupiany R., Amsler M. and Garcia C., 2007. Calibration of an ADP to Estimate Suspended Sand Concentrations in a Large River, Proceedings of Hydraulic Measurements & Experimental Methods 2007, Lake Placid, NY.

U.S. Army Corps of Engineers, 2008. HEC-RAS River Analysis System, Hydraulic Reference Manual.

van Rijn L.C., 1984. Part II: Suspended load transport, Journal of Hydraulic Engineering, 110(11), 1613-1641.

Yalin M. S., da Silva A.M.F., 2001. Fluvial Processes. IAHR Monograph.